Available online at www.sciencedirect.com

SciVerse ScienceDirect

Ceramics International 39 (2013) 8159–8164

CERAMICS INTERNATIONAL

www.elsevier.com/locate/ceramint

Preparation and characterization of $Lu_2SiO_5:Ce^{3+}$ luminescent ceramic fibers via electrospinning

Qi Lu[a,b], Qian Liu[a,*], Qinhua Wei[a,b], Guanghui Liu[a], Jiandong Zhuang[a]

[a]*State Key Laboratory of High Performance Ceramics and Superfine Microstructure, Shanghai Institute of Ceramics, Chinese Academy of Sciences, Shanghai 200050, PRChina*

[b]*Graduate University of Chinese Academy of Sciences, Beijing 100049, PRChina*

Received 11 February 2013; received in revised form 28 March 2013; accepted 29 March 2013
Available online 9 April 2013

Abstract

Cerium-doped lutetium oxyorthosilicate ($Lu_2SiO_5:Ce^{3+}$, or shortly LSO:Ce) luminescent ceramic fibers were synthesized by the sol–gel process followed with electrospinning in the present research. Polyvinyl butyral (PVB) was used as a spinnable carrier and anhydrous system availed the efficient generation of the composite fibers. The phase of Lu_2SiO_5 starts to appear at 1100 °C based on XRD analysis. After annealed at 1200 °C for 4 h, all samples with different cerium doping concentrations show a pure phase of LSO with a well-crystallized structure. The annealed samples retain smooth surfaces and uniform morphologies. LSO:Ce fibers thus prepared exhibit a strong emission peak located at about 403 nm, corresponding to the Ce^{3+} $5d^1 \rightarrow 4\,f^1$ transitions. LSO:1%Ce fibers exhibit the most intense emission among the samples doped with different cerium concentrations, which also present a much stronger emission than that of LSO:1%Ce powders. X-ray excited luminescence (XEL) spectrum shows that LSO:Ce fibers present a considerable scintillation property as well. Short decay time trait was also observed in LSO:Ce fibers due to their microscopic defects at grain boundaries and surfaces.
© 2013 Elsevier Ltd and Techna Group S.r.l. All rights reserved.

Keywords: Lutetium oxyorthosilicate; Electrospinning; Fibers; Luminescence

1. Introduction

Rare earth (RE) compounds have been widely investigated for their optical and luminescence properties, in view of their extensive applications in the fields of high-performance luminescent devices, scintillator materials, field-emission display (FED), and other functional materials [1–3]. Recently, with great progress of nanomaterials fabrication, one-dimensional optical materials, such as nanowires and nanotubes, have attracted great interests as the fundamental blocks for building various optoelectronic nano-devices, nano-lasers, sensors, polarized luminescence, etc [4–7].

The optical properties of one-dimensional materials are closely related with their morphology or structure, due to their high surface to volume ratio and quantum confinement effects. Hou et al. synthesized $CaWO_4$ and $CaWO_4:Tb^{3+}$ one-dimensional nanomaterials by electrospinning. The nanotube samples exhibited higher cathodoluminescence intensity than the nanowire samples [8]. Lieber et al. characterized the high polarized photoluminescence from a single indium phosphide nanowire, whose excellent properties were demonstrated as high resolution, nanoscale photodetectors [9]. Other recent findings presented the film of oriented Gd_2O_3:Eu platelet crystallites showed much stronger emission than that of irregular Gd_2O_3:Eu powders [10], and the RE-Y_2SiO_5 microbelt phosphors also showed a higher emission intensity than that of nanofiber phosphors [11]. Including the results mentioned above, it is also expected that the unique morphology and structure can improve not only the luminescence quantum yield, but also the resolution of display.

$Lu_2SiO_5:Ce^{3+}$ (LSO:Ce), as a scintillating or luminescent material, has increasingly stepped into the spotlight for the field of computerized tomography (CT), positron emission tomography (PET), and environmental monitoring [12,13], owing to its high effective atomic number, outstanding scintillation light yield and short decay time properties [1,14]. LSO materials are commonly fabricated in the form of single crystal or powder, in which their property may be restricted to some extents because of limitations from morphology and size. If LSO: Ce fibers could be fabricated,

*Corresponding author. Tel.: +86 21 52412612; fax: +86 21 52412404.
E-mail address: qianliu@sunm.shcnc.ac.cn (Q. Liu).

0272-8842/$ - see front matter © 2013 Elsevier Ltd and Techna Group S.r.l. All rights reserved.
http://dx.doi.org/10.1016/j.ceramint.2013.03.090

there should have been some new findings. Generally speaking, electrospinning is a feasible and versatile method to produce microfibers or nanofibers with uniform diameter, high surface area, and superior directionality [15,16], which are eligible candidates in many fields including catalyst supports, optical communication, chemical sensors, engineering fields, etc. [17–19]. Such one dimensional morphology may make a special effect when shifted to LSO: Ce fibers for potential applications in nanofiber lasers, optoelectronic nano-devices, ray detectors, optical conversion wrapping materials and even the raw materials for crystal growth. On the basis of our knowledge, silicate fibers only like cerium-activated lithium silicate glass fibers have been fabricated by a hot-downdraw process for the security application and medical applications of sensors for monitoring and surveillance [20].

In the present work, we proposed to obtain fibrous high performance LSO:Ce fibers by a facile method of electrospinning combined with the sol–gel process, which has not been reported before. The crystallinity, morphology and photoluminescent properties of LSO:Ce fibers were investigated. The discovery of strong emission and short decay from LSO:Ce fibers was also reported.

2. Experiment

2.1. Preparation

First, 11.67 mmol Lu_2O_3 was dissolved in concentrated HNO_3 (with a purity of 99.99%, Shanghai Yuelong New Material Chemical Ltd.) under stirring, followed with evaporation by heating to obtain $Lu(NO_3)_3$ solid powders. Then $Lu(NO_3)_3$ powders and a certain amount of $Ce(NO_3)_3$ powders (≧99%, A.R., Sinopharm Chemical Reagent Co., Ltd.) were added simultaneously into ethanol. In addition, a silica sol was prepared by adding 5 g TEOS (tetraethyl orthosilicate $Si(OC_2H_5)_4$, A.R., Shanghai Lingfeng Chemical Reagent Ltd.) in ethanol and deionized water (weight ratio of TEOS:ethanol:H_2O = 1:2:0.4). A few drops of HCl were added into the mixed TEOS–ethanol–H_2O solution for acceleration of hydrolysis with stirring at room temperature for 2 h, with a resultant of viscous sol. Soon afterward, the above $Lu(NO_3)_3$–$Ce(NO_3)_3$-containing solution and a certain amount of PVB (where the weight percentage of PVB is 5% of the total content of water and ethanol in the final mixture solution) were added into the sol. A homogeneous hybrid solution was finally obtained after 2 h agitation for further electrospinning. The above viscous solution was loaded into a hypodermic syringe with a stainless steel needle having an inner diameter of 0.51 mm. The anode of high voltage power supply was clamped to the needle tip, and the cathode was connected to a grounded copper drum covered with an aluminum foil. The applied voltage was 15 kV, and the distance between the needle and collector was 12 cm. Finally, the as-electrospun precursor fibers were annealed at a range of 1000–1200 °C for 4 h in air with heating rate kept to 5 °C/min. Thus, LSO:xCe [$(Lu_{1-x}Ce_x)_2SiO_5$] fibers with varied Ce^{3+} concentration (x = 0.1, 0.25, 0.5, 1.0, and 2.0 at %), were successfully synthesized by the electrospinning method followed by high temperature treatment.

2.2. Characterization

The crystalline structure of the samples was characterized by X-ray diffraction (XRD) with Cu Kα radiation (λ = 0.1541 nm, a D/MAX-2550V X-ray diffractometer working at 40 kV and 100 mA). The size and morphology of electrospun fibers were observed by scanning electron microscopy (SEM, JSM-6510). Thermogravimetric and differential scanning calorimetry analysis were recorded with a thermal analysis instrument (TG–DSC, NETZSCH 409PC). Transmission electron microscope (TEM), high-resolution transmission electron microscope (HRTEM) and selected area electron diffractometer (SAED) micrographs were obtained from a JEM-2100F transmission electron microscope with a field emission gun operating at 200 kV. The photoluminescence measurements (PL) were performed on a Hitachi F-4600 spectrophotometer equipped with a 150 W xenon lamp as the excitation source. The XEL spectra were measured on an X-ray excited spectrometer, FluoMain, where a F-30 movable clinical X-ray tube (W anticathode target) was used as the X-ray source, and operated under the same conditions (30 kV, 4 mV) at room temperature. The decay time curves were measured with the Jobin Yvon Fluorolog-3 spectrofluorometer. All measurements were performed at room temperature.

3. Results and discussion

The XRD patterns of undoped LSO fibers annealed at different temperatures from 1000 to 1200 °C are shown in Fig. 1. When the precursor sample is annealed at 1000 °C, diffraction peaks of $Lu_2Si_2O_7$ indexed to the JCPDS card no. 35-0326 appear on a large scale, while several weaker diffraction peaks are ascribed to the phase of Lu_2SiO_5. When the precursors are annealed at higher temperatures of 1100 °C and 1200 °C, well defined diffraction peaks show up, all of which corresponding to Lu_2SiO_5 phase match with the indexes of JCPDS card no. 41-0239. The average grain sizes of the sample treated at 1100 °C and 1200 °C were estimated from the Scherrer's equation, where diffraction data in the (211), (013), (220), ($\bar{4}$02) planes were taken to calculate.

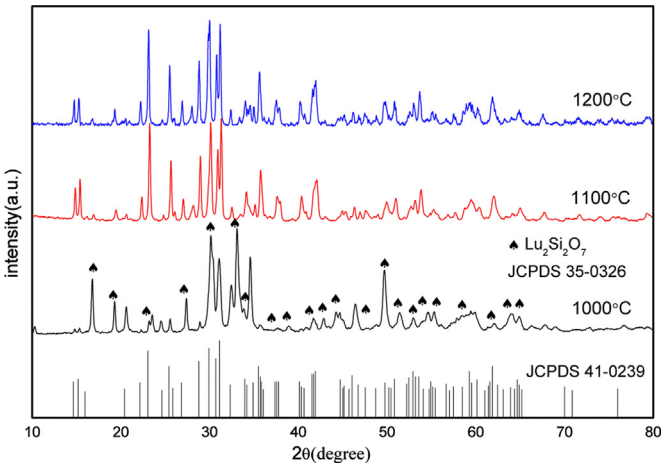

Fig. 1. X-ray diffraction patterns for LSO fibers annealed at 1000–1200°C for 4 h.

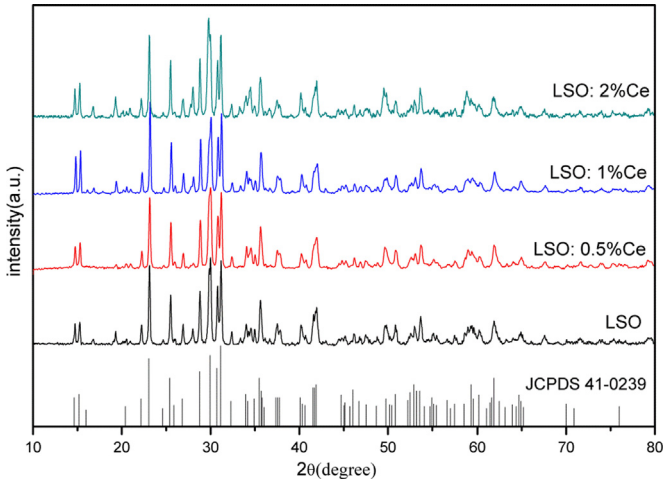

Fig. 2. X-ray diffraction patterns for LSO:Ce fibers with different cerium doping concentrations annealed at 1200 °C for 4 h.

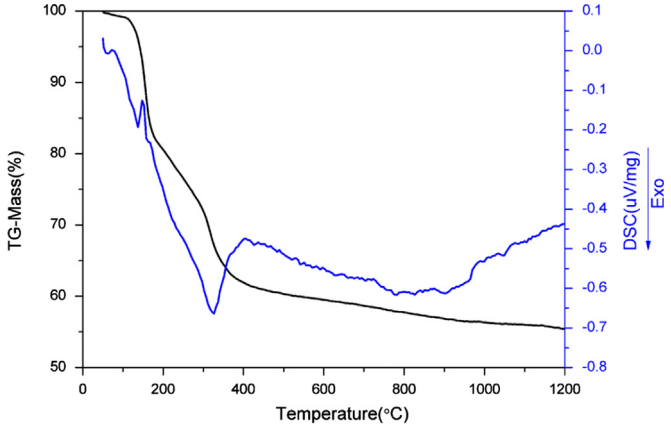

Fig. 3. TG–DSC curves of composite fiber precursor of PVB/LSO:1%Ce.

The estimated average crystallite sizes are 25.1 nm for the sample treated at 1100 °C and 30.2 nm for 1200 °C, respectively. Obviously the sample annealed at 1200 °C presents a higher degree of crystallinity and larger crystallite size. It is consistent with the general rule that the crystallite size increases with the temperature increasing.

The XRD patterns of LSO:Ce fibers doped with various Ce concentrations and annealed at 1200 °C for 4 h are shown in Fig. 2. All products obtained at such a higher temperature 1200 °C own a high degree of crystallinity. Compared to the indexes on JCPDS card no. 41-0239, the XRD patterns of LSO:Ce fibers correspond to the Lu_2SiO_5 phase. Few impurity phases appearing in some of LSO:Ce samples are $Lu_2Si_2O_7$ phases. The existed $Lu_2Si_2O_7$ phases may attribute to the slight deviation of the hydrolysis degree of the sol–gel process, which is sensitively influenced by the temperature and stirring speed in the preparation routes.

Fig. 3 shows a typical thermal behavior of LSO:1%Ce fiber precursors characterized by TG and DSC analyses with a heating rate of 5 °C/min. The weight loss of PVB-containing LSO:Ce precursor exhibits a whole degradation process consisting of three steps as follows: ~20 wt% of weight loss taking place below 180 °C, ~20 wt% of weight loss between 200 °C and 400 °C, and ~5 wt% between 400 °C and 1200 °C. The weight loss at the first step before 200 °C is mainly derived from the evaporation of remaining solvents like water and alcohol. The second step loss between 200 °C and 400 °C ascribes to the decomposition of organic species such as PVB and TEOS. The relatively flat third step after 400 °C corresponds to a further degradation of unsaturated backbone residues and the formation of LSO:Ce [21]. As the DSC curves show, the sharp exothermic peak centered at 327 °C is related to the oxidation and decomposition of PVB. And a broad exothermic peak at 800–1100 °C corresponds to the crystallization and formation of LSO phase.

A SEM image of the as-prepared precursor LSO:1%Ce, a kind of hybrid fibers, is shown in Fig. 4a, as well as the sample treated at 1200 °C shown in Fig. 4b. Although annealed at high temperature, the surface morphology is well reserved. It can be seen that the precursor fibers own a uniform and completely smooth fiber morphology with an average diameter ranging from 500 nm to 2 μm, as presented in Fig. 4b. The phenomenon of shrinkage and curl of fibers can also be observed due to the decomposition of PVB additive and crystallization of the LSO phase.

The TEM and HRTEM images of LSO:Ce fibers are shown in Fig. 4c and Fig. 4d, respectively. The TEM image shows a smooth and homogeneously distributed morphology. A typical HRTEM image clearly shows LSO:Ce fibers with well-resolved lattice fringes. The interplanar spacing of 0.35 nm corresponds to the (202) plane of LSO:Ce crystalline structure. Few grain boundaries and defects are observed in HRTEM and the fibers present high crystallinity and directionality, which further confirms the formation of crystalline LSO:Ce, agreeing well with the XRD analysis results. The SAED pattern in Fig. 4e is indexed and clear unified diffraction patterns can be observed. It could be deduced that the electrospun fibers own some pseudo single crystal subregions, which helps to build the uniformity and directionality inside of samples.

Fig. 5 shows the PL excitation spectra and emission spectra of LSO:Ce fibers under short wavelength ultraviolet (UV) irradiation. All samples were measured in the same condition. The shapes of excitation spectra of LSO:Ce fibers with five different cerium doping concentrations (0.1, 0.25, 0.5, 1.0, and 2.0 at%) are quite similar, composed of three peaks centering at about 263, 300 and 356 nm, which are attributed to the Ce^{3+} $4f^1 \rightarrow 5d^1$ transitions. The PL emission spectra of LSO:Ce fibers were recorded at room temperature by fixing the excitation wavelength at 356 nm. As the Ce^{3+} concentration increases, the intensity of emission at 403 nm increases gradually to a peak value until the Ce^{3+} concentration reaches up to 1.0 at%. And then the intensity decreases owing to the emission quenching from a heavier doping concentration up to 2.0 at%. In comparison, the LSO:1%Ce powders were also prepared by the sol–gel process using the same chemicals and processing as a parallel experiment. Obviously LSO:1%Ce fibers exhibit a stronger emission than that of LSO:1%Ce powders as the dashed light blue lines shown in Fig. 5. Generally, defects which provide non-radiative recombination

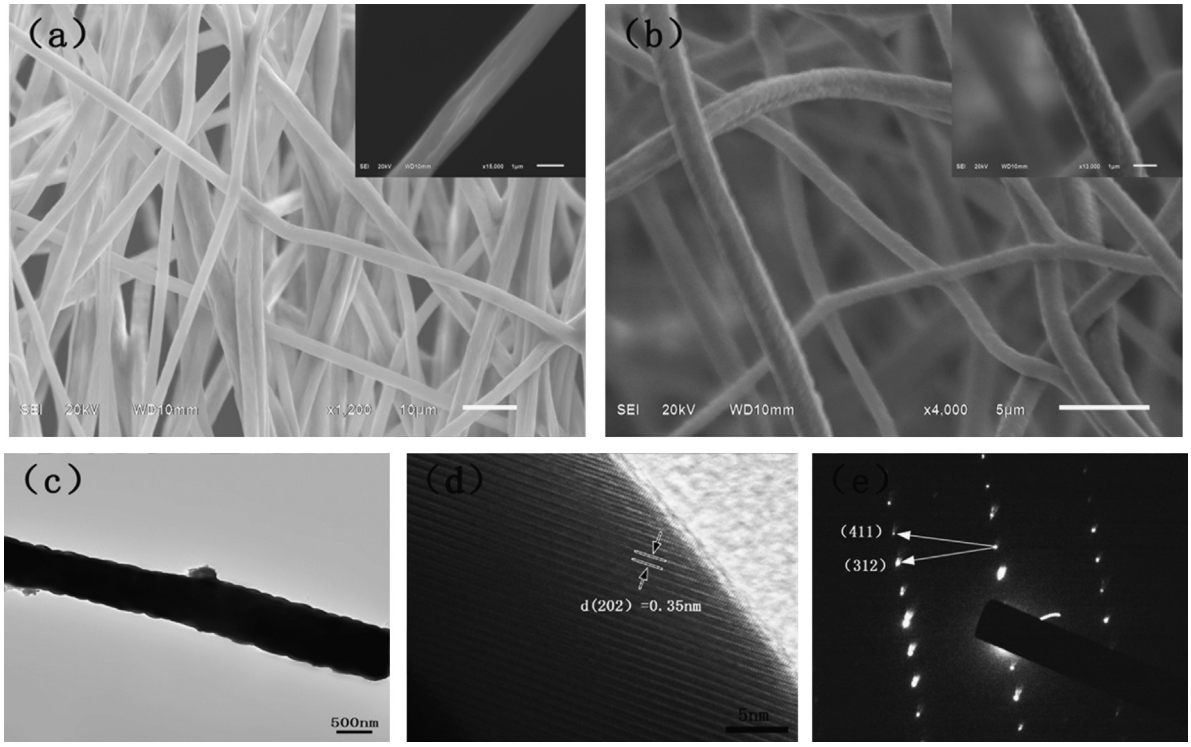

Fig. 4. SEM image of the precursor LSO:1%Ce fibers (a); SEM, TEM, HRTEM images, and SAED of LSO:1%Ce fibers annealed at 1200 °C (b, c, d, e), respectively.

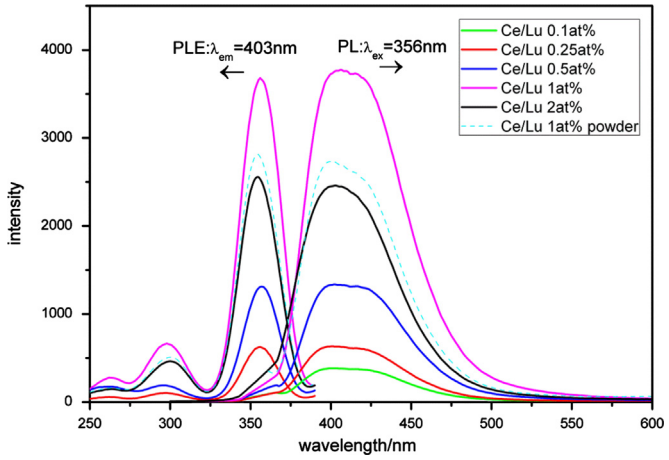

Fig. 5. The PLE and PL curves of LSO:Ce with different cerium doping concentrations. (For interpretation of the references to color in this figure legend, the reader is referred to the web version of this article.)

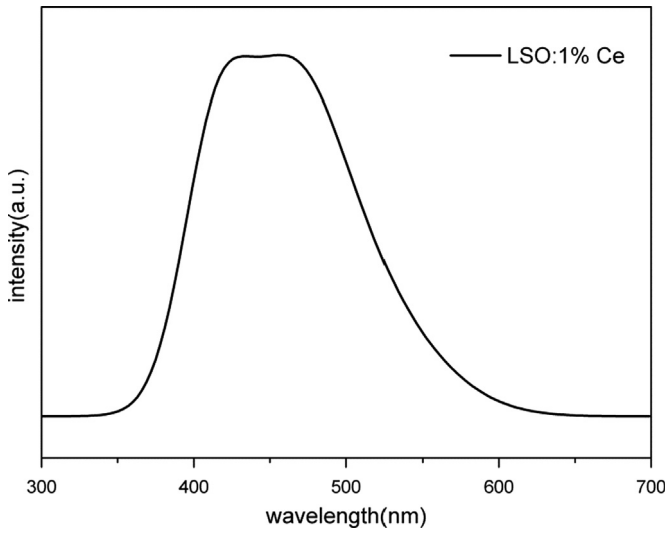

Fig. 6. X-ray excited luminescence of LSO:1%Ce fibers at room temperature.

routes for electrons and holes have a serious drawback in PL intensity for phosphors. Such a phenomenon may refer to less defects on fiber surface or in fiber body than those endowed by powders, which could be attributed to better crystallinity and less aggregation in fibers [22].

The X-ray excited luminescence (XEL) spectrum of LSO:1%Ce fiber samples is presented in Fig. 6. The shape of curve is similar with the PL spectra excited by UV. It is obvious that the emission curve is not symmetrical at its both sides, owning a doublet structure with a long tail on the right-hand side. Suzuki et al. [23], once proposed that LSO lattice contains two sites, Ce1 and Ce2, for Lu ions with 6 and 7 oxygen ligands. According to the reports of Ren et al. [24], its doublet structure of the spectra can be associated with the transition of the Ce^{3+} ions at Ce1 site from the lowest 5d level to the two 4f ground states. And the broad wavelength band on the right-hand side should be ascribed to the transitions at Ce2. Compared with the spectra excited by UV, the obvious red-shift phenomenon occurs in the spectrum excited by X-ray. It is caused by different energy transfer mechanism between excitation of X-ray and UV. When excited by X-ray, the energy is absorbed by LSO matrix and then transferred to Ce^{3+}

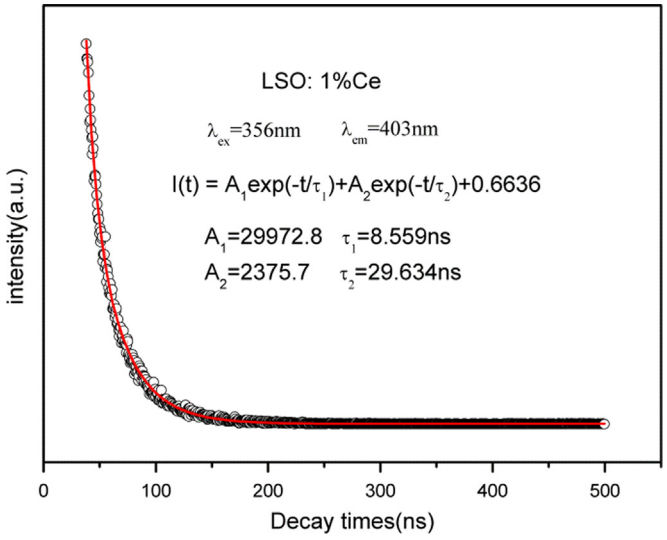

Fig. 7. Decay time curve for the luminescence of LSO:1%Ce fibers.

for the luminescence process [23]. Energy will be released in the form of non-radiative transition when encountering the defects in the matrix. Differently, the UV directly excites the Ce^{3+} without such a process so that the red-shift phenomenon occurs when excited by X-ray. This result shows LSO:Ce fibers present a considerable scintillation property, which provide great potential for LSO:Ce fibers to be used as optical fibers for sensors or ray detectors.

The photoluminescence decay curve of sample LSO:1%Ce is shown in Fig. 7. The decay curve can be well fitted into a double exponential function as $I = A1\exp(-t/\tau_1) + A2\exp(-t/\tau_2)$ under the 403 nm emission of Ce^{3+}, deriving with two lifetimes, a slow one, $\tau_1 = 29.63$ ns, and a fast one, $\tau_2 = 8.56$ ns. But the fast one dominates the amount for 92.7%. It has been previously demonstrated that there exists no fast decay time at a several-nanosecond level for LSO single crystals and the fitted value illustrated in Fig. 7 is much smaller than the theoretical value 40 ns. The fast proportion is deemed to originate from surface and grain boundary effect of polycrystalline fibers. The grain boundaries and defects which own the composite centers of electrons and holes provide the environment for composite annihilation of electron–hole pair in a very short time [25]. Consequently, the successful synthesis of LSO:1% Ce fibers provides a possibility for fabricating one-dimensional fast scintillators or devices.

4. Conclusion

In summary, one-dimensional cerium-doped lutetium oxyorthosilicate (LSO:Ce) luminescent ceramic fibers have been successfully synthesized by electrospinning in conjunction with the sol–gel process. After annealing the precursors at 1200 °C for 4 h, the pure phase of LSO was obtained with a well-crystallized structure and the fibers maintain smooth surface and uniform morphology. PL measurement presents that LSO:Ce fibers show a strong emission peak at about 403 nm corresponding to the Ce^{3+} $5d^1 \rightarrow 4f^1$ transitions. The most intense emission is observed in LSO:1%Ce fibers. And the LSO:1%Ce fibers also show a stronger light emission than that of LSO:1%Ce powders with same chemical composition. Red-shift phenomenon occurs in the spectrum excited by X-ray compared with UV. A short decay time of several nanoseconds is also detected. Such luminescent ceramic LSO:Ce fibers with strong emission and short decay have prosperous applications in the fields of optoelectronic and optical nano-devices, ray detectors, sensors, optical conversion wrapping materials and even the raw materials for crystal growth.

Acknowledgments

We gratefully acknowledge the financial support by the National Natural Science Foundation of China (No.91022028) and by the State Key Lab of High Performance Ceramic and Superfine Microstructure, Shanghai Institute of Ceramics (No. O81GS1181G).

References

[1] C. Mansuy, F. Leroux, R. Mahiou, J. Nedelec, Preferential site substitution in sol-gel derived Eu^{3+} doped Lu_2SiO_5: A combined study by X-ray absorption and luminescence spectroscopies, Journal of Materials Chemistry 15 (38) (2005) 4129–4135.

[2] H. Song, H. Yu, G. Pan, X. Bai, B. Dong, X.T. Zhang, S.K. Hark, Electrospinning preparation, structure, and photoluminescence properties of YBO_3:Eu^{3+} nanotubes and nanowires, Chemistry of Materials 20 (14) (2008) 4762–4767.

[3] R.J. Xie, M. Mitomo, K. Uheda, F.F. Xu, Y. Akimune, Preparation and luminescence spectra of calcium- and rare-earth (R=Eu, Tb, and Pr)-codoped alpha-SiAlON ceramics, Journal of the American Ceramic Society 85 (5) (2002) 1229–1234.

[4] C. Giansante, G. Raffy, C. Schaefer, H. Rahma, M.T. Kao, A.G.L. Olive, A. Del Guerzo, White-light-emitting self-assembled nanofibers and their evidence by microspectroscopy of individual objects, Journal of the American Chemical Society 133 (2) (2011) 316.

[5] B. Simpkins, P. Pehrsson, M. Taheri, R. Stroud, Diameter control of gallium nitride nanowires, Journal of Applied Physics 101 (9) (2007) 094305-094305-094305.

[6] Z. Fan, D. Dutta, C.J. Chien, H.Y. Chen, E.C. Brown, P.C. Chang, J.G. Lu, Electrical and photoconductive properties of vertical ZnO nanowires in high density arrays, Applied Physics Letters 89 (21) (2006) 213110–213113.

[7] J.C. Johnson, H.J. Choi, K.P. Knutsen, R.D. Schaller, P. Yang, R.J. Saykally, Single gallium nitride nanowire lasers, Nature Materials 1 (2) (2002) 106–110.

[8] Z. Hou, C. Li, J. Yang, H. Lian, P. Yang, R. Chai, Z. Cheng, J. Lin, One-dimensional $CaWO_4$ and $CaWO_4$:Tb^{3+} nanowires and nanotubes: electrospinning preparation and luminescent properties, Journal of Materials Chemistry 19 (18) (2009) 2737.

[9] J.F. Wang, M.S. Gudiksen, X.F. Duan, Y Cui, C.M Lieber, Highly polarized photoluminescence and photodetection from single indium phosphide nanowires, Science 293 (5534) (2001) 1455–1457.

[10] K.H. Lee, B.I. Lee, J.H. You, S.H. Byeon, Transparent Gd_2O_3:Eu phosphor layer derived from exfoliated layered gadolinium hydroxide nanosheets, Chemical Communications 46 (9) (2010) 1461–1463.

[11] L. Wang, Z. Hou, Z. Quan, C. Li, J. Yang, H. Lian, P. Yang, J. Lin, One-dimensional Ce^{3+} and/or Tb^{3+}-doped X1-Y_2SiO_5 nanofibers and microbelts: electrospinning preparation and luminescent properties, Inorganic chemistry 48 (14) (2009) 6731–6739.

[12] P. Dorenbos, C. Van Eijk, A. Bos, C. Melcher, Afterglow and thermoluminescence properties of Lu_2SiO_5:Ce scintillation crystals, Journal of Physics: Condensed Matter 6 (22) (1999) 4167.
[13] C. Yan, G. Zhao, Y. Hang, L. Zhang, J. Xu, Comparison of cerium-doped $Lu_2Si_2O_7$ and Lu_2SiO_5 scintillators, Journal of Crystal Growth 281 2 (2005) 411–415.
[14] L. Pidol, O. Guillot-Noël, A. Kahn-Harari, B. Viana, D. Pelenc, D. Gourier, EPR study of Ce^{3+} ions in lutetium silicate scintillators $Lu_2Si_2O_7$ and Lu_2SiO_5, Journal of Physics and Chemistry of Solids 67 (4) (2006) 643–650.
[15] M.V. Kakade, S. Givens, K. Gardner, K.H. Lee, D.B. Chase, J.F. Rabolt, Electric field induced orientation of polymer chains in macroscopically aligned electrospun polymer nanofibers, Journal of the American Chemical Society 129 (10) (2007) 2777–2782.
[16] W. Li, C.Y. Cao, C.Q. Chen, Y. Zhao, W.G. Song, L. Jiang, Fabrication of nanostructured metal nitrides with tailored composition and morphology, Chemical Communications 47 (12) (2011) 3619–3621.
[17] L. Huang, L. Cheng, H. Yu, J. Zhang, L. Zhou, J. Sun, H. Zhong, X. Li, Y. Tian, Y. Zheng, Electrospinning preparation and optical transition properties of Eu $(DBM)_3$Phen/PS fluorescent composite fibers, Optics Communications 285 (2012) 1476–1480.
[18] Z. Hou, P. Yang, C. Li, L. Wang, H. Lian, Z. Quan, J. Lin, Preparation and luminescence properties of YVO_4:Ln and $Y(V,P)O_4$:Ln (Ln=Eu^{3+}, Sm^{3+}, Dy^{3+}) nanofibers and microbelts by sol–gel/electrospinning process, Chemistry of Materials 20 (21) (2008) 6686–6696.
[19] L.L. Wang, X.M. Liu, Z.Y. Hou, C.X. Li, P.P. Yang, Z.Y. Cheng, H.Z. Lian, J. Lin, Electrospinning synthesis and luminescence properties of one-dimensional Zn_2SiO_4:Mn^{2+} microfibers and microbelts, Journal of Physical Chemistry C 112 (48) (2008) 18882–18888.
[20] R. Seymour, B. Richardson, M. Morichi, M. Bliss, R. Craig, D. Sunberg, Scintillating-glass-fiber neutron sensors, their application and performance for plutonium detection and monitoring, Journal of Radioanalytical and Nuclear Chemistry 243 (2) (2000) 387–388.
[21] X. Zhou, Y. Zhao, X. Cao, Y. Xue, D. Xu, L. Jiang, W. Su, Fabrication of polycrystalline lanthanum manganite ($LaMnO_3$) nanofibers by electrospinning, Materials Letters 62 (3) (2008) 470–472.
[22] Y. Gu, Q. Zhang, H. Wang, Y. Li, $CaSi_2O_2N_2$:Eu nanofiber mat based on electrospinning: facile synthesis, uniform arrangement, and application in white LEDs, Journal of Materials Chemistry 21 (44) (2011) 17790.
[23] H. Suzuki, T.A. Tombrello, C.L. Melcher, J.S. Schweitzer, UV and gamma-ray excited luminescence of cerium-doped rare-earth oxyorthosilicates, Nuclear Instruments & Methods in Physics Research Section A: Accelerators, Spectrometers, Detectors and Associated Equipment 320 (1-2) (1992) 263–272.
[24] G. Ren, L. Qin, S. Lu, H. Li, Scintillation characteristics of lutetium oxyorthosilicate (Lu_2SiO_5:Ce) crystals doped with cerium ions, Nuclear Instruments and Methods in Physics Research Section A: Accelerators, Spectrometers, Detectors and Associated Equipment 531 (3) (2004) 560–565.
[25] J. Xie, T. Lin, Y. Shi, G. Song, W. Wu, Luminescence properties of nano-sized Lu_2SiO_5:Ce phosphors prepared by sol-gel method, Journal of the Chinese Ceramic Society 10 (2010) 018.